Journal of Enzyme Inhibition and Medicinal Chemistry

http://informahealthcare.com/enz
ISSN: 1475-6366 (print), 1475-6374 (electronic)

J Enzyme Inhib Med Chem, Early Online: 1–6
 DOI: 10.3109/14756366.2014.1002401

informa
healthcare

RESEARCH ARTICLE

# Synthesis and evaluation of biological and antitumor activities of 5,7-dimethyl- oxazolo[5,4-*d*]pyrimidine-4,6(5*H*,7*H*)-dione derivatives as novel inhibitors of FGFR1

Faqing Ye[1,2], Yuewu Wang[2], Siyun Nian[2], Yu Wang[2], Di Chen[2], Shufang Yu[2], and Sicen Wang[1]

[1]*School of Pharmacy, Health Science Center Xi'an Jiaotong University, Xi'an, China and* [2]*School of Pharmaceutical Sciences, Wenzhou Medical University, Wenzhou, China*

**Abstract**

A series of 5,7-dimethyl-oxazolo[5,4-*d*]pyrimidine-4,6(5*H*,7*H*)-dione derivatives, **N5a–5l**, was designed, synthesized and evaluated for their FGFR1-inhibition ability as well as cytotoxicity against three cancer cell lines (H460, B16F10 and A549) *in vitro*. Several compounds displayed good-to-excellent potency against these cancer cell lines compared to SU5402. Structure–activity relationship analyses indicated that compounds with a rigid structure and more heteroatoms at the side chain of the parent ring were more effective than those without these substitutions. The compound **N5g** (37.4% FGFR1 inhibition at 1.0 μM) was identified to have the most potent antitumor activities, with $IC_{50}$ values of 5.472, 4.260 and 5.837 μM against H460, B16F10 and A549 cell lines, respectively. Together, our results suggest that 5,7-dimethyl-oxazolo[5,4-d]pyrimidine-4,6(5*H*,7*H*)-dione derivatives may serve as potential agents for the treatment of FGFR1-mediated cancers.

**Keywords**

Cancer therapy, FGFR1, kinase inhibitor, structure–activity relationship, synthesis

**History**

Received 29 October 2014
Revised 26 November 2014
Accepted 30 November 2014
Published online 16 February 2015



## Introduction

Cancer is a major health concern in today's society due to increasing instances of diagnosis and mortality. Various types of cancer therapeutic drugs are in clinical use, but many of these drugs fail to cure the disease because of their low selectivity and high toxicity[1,2]. In the last decade, receptor tyrosine kinases (RTKs) have become a hot topic in the field of cancer research. There is growing interest in targeting these receptors for cancer therapy[3]. Fibroblast growth factor receptors (FGFR1, FGFR2, FGFR3 and FGFR4) constitute a major class of RTKs serving as high-affinity receptors for a large family of fibroblast growth factors (FGFs) to control key cellular processes, such as cell proliferation, migration and apoptosis[4,5]. FGFRs and their associated FGFs have been receiving increasing attention in the area of antitumor drug discovery[6,7].

FGFR1 is the founding member of FGFR family and is known to be ectopically expressed in prostate carcinoma cells, breast carcinoma cells, lung cancer cells and also other cancer cells[8,9]. Amplification of FGFR1 occurs in 10% of breast cancers and is associated with poor prognosis[10]. Given the pivotal role of FGFR1 in human cancers, we sought to analyze and target the pathway of cancer development through FGFR1 overexpression and/or activation. Previous studies have shown the importance of ATP-binding of FGFR1 for its enzymatic activity[11–13]. The RTKs are catalyzed upon ATP binding to their enzymatic pockets, which aid in the transfer of phosphate from ATP to the tyrosine residues of their target proteins[14]. In the presence of tyrosine kinase inhibitors, cell proliferation would be blocked by preventing the ATP from binding to the RTKs. Our goal was to design a new class of tyrosine kinase inhibitors that can mimic ATP and block the constitutive activation of FGFR1, thereby blocking the FGFR1-dependent cancer signaling pathway.

Through structural analyses of FGFR1 inhibitors, SU5402, PD173074 (Figure 1) and others, we discovered certain criteria that needed to be fulfilled in order to achieve high affinity binding to the FGFR1 ATP binding pocket. These criteria require the parent nucleus of FGFR1 antagonists to be: (i) flat, (ii) aromatic or π–electron-rich and (iii) nitrogen-containing heterocycles[15–20]. SU5402 and PD173074 serve as important antitumor inhibitors because of their good selectivity towards FGFR1. As expected, they both fit within the identified criteria. Molecular docking also reveals that the parent nuclei of SU5402 and PD173074 occupy the same site as ATP adenine, and that their nitrogen interacted with the ATP hinge. However, the 3-position side chain of SU5402 could not completely take up the hydrophobic pocket, which plays an important role in the inhibition of FGFR1. In addition, when testing for inhibition in the growth of BaF3/ZNF198-FGFR1 cells, the $IC_{50}$ of SU5402 was reported to be 5.0 μM, whereas that of PD173074 was 1000 times higher[21]. Furthermore, PD173074 and SU5402 failed to enter phase II clinical trials because of their high toxicity[22,23].

Herein we have adopted a nonconventional strategy to design a lead compound (Figure 1), which contains more heteroatoms, and resulted in the formation of an intermolecular hydrogen bond in the ATP binding site. Such exchange of the side chain position facilitated the interaction between the hydrophobic pocket of

Address for correspondence: Sicen Wang, Professor, School of Pharmacy, Health Science Center Xi'an Jiaotong University, Xi'an 710061, China. Tel: +86 29 82656788. Fax: +86 29 82655451. E-mail: wangsc@mail.xjtu.edu.cn

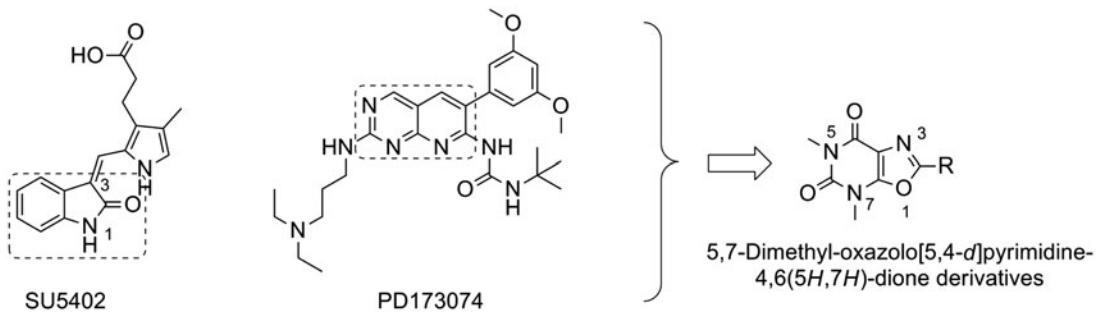


Figure 1. The rationale for the design of the target compounds.



FGFR1 and the compounds resulting in higher binding affinity. A core scaffold 5,7-dimethyl-oxazolo[5,4-*d*]pyrimidine-4,6(5*H*,7*H*)-dione was selected based on the substructure similarity, which is rarely reported in the field of RTK inhibitors with antitumor activity. Additionally, the 2-position was also substituted with different aromatic derivatives based on SAR. Our main goal was to determine whether the 5,7-dimethyl-oxazolo[5,4-*d*]pyrimidine-4,6(5*H*,7*H*)-dione derivatives were able to confer higher potency against cancer cells and to search for a new heterocyclic stem nucleus that contributes to the design of novel antitumor drugs.

## Materials and methods

### Experimental section

Experimental: Melting points (uncorrected values): METTLER TOLEDO XRC-1 micro-melting point apparatus (Shanghai, China). Infrared Spectroscopy (IR): Perkin-Elmer FT-IR 1605 spectrometer (Nicolet, America). $^1$H NMR spectra: Bruker Avance-3600 spectrometer (600 MHz) (Waldbronn, Germany). Samples were dissolved in $CDCl_3$ or $d_6$-DMSO, while tetramethylsilane (TMS) was used as an internal standard. Mass spectra (MS): Agilent-1100 LC mass spectrometer (Waldbronn, Germany). Analytical thin layer chromatography (TLC, $R_f$ values) was performed on Silica Gel plates $F_{254}$ (0.2-mm thick) and visualization of the spots was effected by exposure to UV light. These apparatus were provided by Wenzhou Medical University.

*General procedure for the synthesis of 1,3-dimethyl-5-nitroso-pyrimidine-2,4,6(1H,3H,5H)-trione (**2**):* 1,3-Dimethyl-pyrimidine-2,4,6(1*H*,3*H*,5*H*)-trione (**1**) (0.03 mol) was added to a mixture of acetic acid (70 ml) and water (70 ml). The mix solution was stirred for 1 h at 75 °C, and then cooled to 50 °C. Then $NaNO_2$ (0.06 mol) was added in batches to the reaction mixture stirring for 1 h and recooled to room temperature. Then the deposit was filtered and washed with water, dried, concentrated *in vacuo* to obtain the white solid product 1,3-dimethyl-5-nitroso-pyrimidine-2,4,6 (1*H*, 3*H*, 5*H*)-trione (**2**) with yields of 81%.

*General procedure for the synthesis of 1,3-dimethyl-5-amino-pyrimidin-2,4,6(1H,3H,5H) –trione (**3**):* Compound **2** (0.01 mol) was added to a mixture of 14.5% $NH_4OH$ (14 ml) and then $Na_2S_2O_4$ (0.02 mol) was added in batches. The solution was refluxed for 30 min at 50 °C. After removing the ammonia water by reduced pressure distillation, the filtrate was washed with water and dried to get the white solid product 1,3-dimethyl-5-amino-pyrimidin-2,4,6(1*H*,3*H*,5*H*)-–trione (**3**) in 80% yield.

*General procedure for the synthesis of imines (**4a–l**)*: **3** (0.001 mol) and the aromatic aldehyde (0.001 mol) were added to 15 ml ethanol. Then the mixture was refluxed for 3 h at 80 °C and cooling to 0 °C. The filtrate was washed with water and dried to produce intermediate white solid product (**4a**–**l**) in 50–70% yield.

*General procedure for the synthesis of imines (**N5a–l**)*: Compounds **4a**–**l** (0.01 mol) were added to 1.5 ml thionyl chloride and the solution was refluxed for 1 h at 60 °C. After removing the thionyl chloride by reduced pressure distillation, the mixture was dissolved in a little of water. Then adjust to pH 7 by ammonia water. They were purified by further recrystallization with DMSO:ethanol = 1:1 and dried to get the target compound 5,7-dimethyl-oxazolyl[5,4-*d*]pyrimidine-4,6(5*H*,7*H*)-dione derivatives (**N5a–l**).

*2-(Furan-2-yl)-5,7-dimethyl-4H-oxazolo[5,4-d]pyrimidine-4,6 (5H,7H)-dione (**N5a**)*: Yield: 45.5%. White solid, mp: 185–187 °C. IR (KBr), cm$^{-1}$: 1717, 1682 (C = O); $^1$H NMR ($CDCl_3$) $\delta$(ppm): 3.50 (s, 3H, $N^5$–$CH_3$), 3.70 (s, 3H, $N^7$–$CH_3$), 6.58–6.63 (m, 1H, 4′furan-H), 7.14 (s, 1H, 3′furan-H), 7.60 (s, 1H, 5′furan-H). EI-MS: 248.2[M+H]$^+$.

*2-(Thiophen-2-yl)-5,7-dimethyl-4H-oxazolo[5,4-d]pyrimidine-4,6(5H,7H)-dione (**N5b**)*: Yield: 52.1%. White solid, mp: 198–200 °C. IR (KBr), cm$^{-1}$: 1717, 1679 (C = O). $^1$H NMR (DMSO-$d_6$) $\delta$(ppm): 3.45 (s, 3H, $N^5$–$CH_3$), 3.65 (s, 3H, $N^7$–$CH_3$), 7.15–7.22 (m, 1H, 4′thiophene-H), 7.52 (d, 1H, 3′thiophene-H, $J$ = 4.2 Hz), 7.75 (d, 1H, 5′thiophene-H, $J$ = 4.2 Hz). EI-MS: 264.5[M+H]$^+$.

*2-(Pyridin-2-yl)-5,7-dimethyl-4H-oxazolo[5,4-d]pyrimidine-4, 6(5H,7H)-dione (**N5c**)*: Yield: 54.7%. White solid, mp: 197–200 °C. IR (KBr), cm$^{-1}$: 1718, 1622 (C = O). $^1$H NMR ($CDCl_3$) $\delta$(ppm): 3.47 (s, 3H, $N^5$–$CH_3$), 3.71 (s, 3H, $N^7$–$CH_3$), 7.16–7.22 (m, 1H, 5′pyridine-H), 7.43–7.47 (m, 1H, 4′pyridine-H), 7.51–7.62 (m, 1H, 3′pyridine-H), 7.65 (s, 1H, 6′pyridine-H). EI-MS: 258.7[M+H]$^+$.

*2-[(4-Benzyloxy)phenyl]-5,7-dimethyl-4H-oxazolo[5,4-d]pyrimidine-4,6(5H,7H)-dione (**N5d**)*: Yield: 60.3%. White solid, mp: 220–222 °C. IR (KBr), cm$^{-1}$: 1714, 1667 (C = O). $^1$H NMR ($CDCl_3$) $\delta$(ppm): 3.45 (s, 3H, $N^5$–$CH_3$), 3.64 (s, 3H, $N^7$–$CH_3$), 5.13 (s, 2H, –$OCH_2$), 7.06 (d, 2H, phenyl-H, $J$ = 9.0 Hz), 7.32–7.38 (m, 1H, phenyl-H), 7.40 (d, 2H, phenyl-H, $J$ = 7.8 Hz), 7.43 (d, 2H, phenyl-H, $J$ = 7.2 Hz), 7.9 (d, 2H, phenyl-H, $J$ = 9.0 Hz). EI-MS: 364.0[M+H]$^+$.

*2-[(4-Piperidin-1-yl)phenyl]-5,7-dimethyl-4H-oxazolo[5,4-d] pyrimidine-4,6(5H,7H)-dione (**N5e**)*: Yield: 46.7%. Light yellow solid, mp: 221–223 °C. IR (KBr), cm$^{-1}$: 1717, 1676 (C = O). $^1$H NMR ($CDCl_3$) $\delta$(ppm): 1.65–1.75 (m, 6H, piperidine-H), 3.20–3.38 (m, 4H, piperidine-H), 3.40 (s, 3H, $N^5$–$CH_3$), 3.60 (s, 3H, $N^7$–$CH_3$), 6.86 (d, 2H, phenyl-H, $J$ = 9.0 Hz), 7.87 (t, 2H, phenyl-H, $J$ = 9.0 Hz). EI-MS: 341.2[M+H]$^+$.

*(E)-2-(1-Phenylprop-1-en-2-yl)-5,7-dimethyl-4H-oxazolo[5,4-d]pyrimidine-4,6(5H,7H)-dione (**N5f**)*: Yield: 55.2%. Light yellow solid, mp: 185–187 °C. IR (KBr), cm$^{-1}$: 1682, 1614 (C = O). $^1$H NMR ($CDCl_3$) $\delta$(ppm): 2.45 (s, 3H, –$CH_3$), 3.48 (s, 3H, $N^5$–$CH_3$), 3.68 (s, 3H, $N^7$–$CH_3$), 7.41–7.47 (m, 2H, phenyl-H), 7.52 (s, 1H, CH = C), 7.54–7.65 (m, 3H, phenyl-H). EI-MS: 298.0[M+H]$^+$.

*(E)-2-(4-Methyl-1-phenylpent-1-en-1-yl)-5,7-dimethyl-4H-oxazolo[5,4-d]pyrimidine-4,6-(5H, 7H)-dione (**N5g**)*: Yield: 43.2%. White solid, mp: 184–185 °C. IR (KBr), cm$^{-1}$: 1719, 1638 (C = O). $^1$H NMR (DMSO-$d_6$) $\delta$(ppm): 0.97–1.10

(m, 6H, $CH_3\times2$), 1.78–1.85 (m, 1H, CH), 2.11–2.18 (m, 2H, $CH_2$), 3.25 (s, 3H, $N^5$–$CH_3$), 3.95 (s, 3H, $N^7$–$CH_3$), 7.35 (d, 2H, phenyl-H, $J=7.8$ Hz), 7.48 (t, 1H, phenyl-H, $J=7.8$ Hz), 7.52 (s, 1H, CH = C), 7.88 (t, 2H, phenyl-H, $J=7.8$ Hz).

*2-(3a,7a-Dihydro-1H-indol-3-yl)-5,7-dimethyl-4H-oxazolo[5,4-d] pyrimidine-4,6(5H,7H)-dione (**N5h**)*: Yield: 60%. White solid, mp: 298–300 °C. IR (KBr), $cm^{-1}$: 3227.94 (N–H), 1710, 1674 (C = O). $^1$H NMR (DMSO-$d_6$) $\delta$(ppm): 3.38 (s, 3H, $N^5$–$CH_3$), 3.55 (s, 3H, $N^7$–$CH_3$), 7.15–7.35 (m, 2H, indole-H), 7.53 (d, 1H, indole-H, $J=7.2$ Hz), 8.14 (d, 1H, indole-H, $J=7.2$ Hz), 8.20 (s, 1H, indole-H), 11.97 (s, 1H, indole-H). EI-MS: 297$[M+H]^+$.

*2-(Naphthalen-1-yl)-5,7-dimethyl-4H-oxazolo[5,4-d]pyrimidine-4,6(5H,7H)-dione (**N5i**)*: Yield: 49.1%. White solid, mp: 276–279 °C. IR (KBr), $cm^{-1}$: 1715, 1669 (C = O). $^1$H NMR (DMSO-$d_6$) $\delta$(ppm): 3.34 (s, 3H, $N^5$–$CH_3$), 3.58 (s, 3H, $N^7$–$CH_3$), 7.53–7.69 (m, 2H, naphthnalene-H), 7.99–8.01 (m, 1H, naphthnalene-H), 8.11–8.23 (m, 3H, naphthnalene-H), 8.66 (s, 1H, naphthnalene-H). EI-MS: 308$[M+H]^+$.

*2-(2-Hydroxy-naphthalen-1-yl)-5,7-dimethyl-4H-oxazolo[5,4-d]pyrimidine-4,6(5H,7H)-dione (**N5j**)*: Yield: 57.6%. White solid, mp: 280–282 °C. IR (KBr), $cm^{-1}$: 1718, 1673 (C = O). $^1$H NMR ($CDCl_3$) $\delta$(ppm): 3.50 (s, 3H, $N^5$–$CH_3$), 3.80 (s, 3H, $N^7$–$CH_3$), 7.32 (d, 1H, naphthnalene-H, $J=9.0$ Hz), 7.34–7.44 (m, 1H, naphthnalene-H), 7.63–7.77 (m, 1H, naphthnalene-H), 7.84 (d, 1H, naphthnalene-H, $J=9.0$ Hz), 7.89 (d, 1H, naphthnalene-H, $J=9.0$ Hz), 8.59 (d, 1H, naphthnalene-H, $J=9.0$ Hz), 11.85 (s, 1H, –OH). EI-MS: 323.9$[M+H]^+$.

*2-(Anthracen-9-yl)-5,7-dimethyl-4H-oxazolo[5,4-d]pyrimidine-4,6(5H,7H)-dione (**N5k**)*: Yield: 56.6%. White solid, mp: 275–278 °C. IR (KBr), $cm^{-1}$: 1697, 1684 (C = O). $^1$H NMR ($CDCl_3$) $\delta$(ppm): 3.58 (s, 3H, $N^5$–$CH_3$), 3.66 (s, 3H, $N^7$–$CH_3$), 7.55–7.68 (m, 4H, anthracene-H), 8.04 (d, 2H, anthracene-H, $J=7.8$ Hz), 8.12 (d, 2H, anthracene-H, $J=7.8$ Hz,), 8.71 (s, 1H, anthracene-H); EI-MS: 358.2$[M+H]^+$.

*5,7-Dimethyl-2-quinolin-2-yl-4H-oxazolo[5,4-d]pyrimidine-4, 6(5H,7H)-dione (**N5l**)*: Yield: 59.7%. White solid, mp: 297–299 °C. IR (KBr), $cm^{-1}$: 1717, 1665 (C = O). $^1$H NMR (DMSO-$d_6$) $\delta$(ppm): 3.40 (s, 3H, $N^5$–$CH_3$), 3.66 (s, 3H, $N^7$–$CH_3$), 7.58–7.65 (m, 2H, quinoline-H), 7.42 (d, 2H, quinoline-H, $J=7.8$ Hz), 8.04 (d, 1H, quinoline-H, $J=7.8$ Hz), 8.30 (s, 1H, quinoline-H). EI-MS: 308.9$[M+H]^+$.

### FGFR kinase inhibition assay

FGFR1 kinase activity was determined by LANCE Ultra TR-FRET Assay. For the determination of $IC_{50}$, the compounds were tested in duplicate at three concentrations (10, 1 and 0.1 μM). A standard enzymatic reaction, initiated by transferring 5 μl of compound to one tube and adding of 95 μl of 1 × kinase buffer (50 mM HEPES, pH 7.5, 10 mM $MgCl_2$, 1 mM EGTA, 2 mM DTT, 0.01% Tween-20) in the same tube. As a control, 5 μl of 100% DMSO was transferred to one tube and 95 μl of 1 × kinase buffer was added in the same tube (10-fold dilution by 1 x kinase buffer). Then 2.5 μl from each tube was transferred to the 384-well assay plate, which contains 4 × compounds and positive control SU5402 at the concentration of 10, 1 and 0.1 μM, respectively. Then 2.5 μl of 4 x enzyme solution was added to each well of the assay plate. After 10-min incubation at room temperature, 5 μl of 2.5 × peptide solution (ULight-JAK-1 peptide and ATP in 1 × kinase base buffer) was transferred to each well of the 384-well assay plate followed by additional 60-min incubation at 28 °C. The reaction was stopped by addition of the termination buffer (5 μl of 40 mM EDTA) for 5 min. Finally, 5 μl of 4X antibody (Eu-anti-phospho-tyrosine Antibody (PT66) at a final concentration of 2 nM) was added to each well of the 384-well assay plate and incubated for 1 h. The activity of the tyrosine kinase was detected by the EnVision Multilabel Reader and controlled by SPSS.

### MTT assay for antitumor activity in cellular level

All of tested cancer cells were obtained from Pilot base of Wenzhou Medical College and grown in Dulbecco's Modified Eagle Medium with high glucose. And these media were supplemented with 10% fetal bovine serum, 50 U/ml penicillin and 50 μg/ml streptomycin. All of the tissue culture reagents were purchased from Gino Biomedical Technology Co, Ltd. and cultivated at 37 °C in a humidified incubator with 5% $CO_2$. At the beginning of the assay, these cells (5000/well) were, respectively, cultured in a 96-well microplate for 1 day. Then the cells were treated with 100 μl of new medium (SU5402 as positive control group 0.2, 4, 10, 50 μg/ml) containing the test substances. After incubation for 24 h, 20 μg/ml of 3 -(4,5-dimethylthiazol-2-yl)-2,5-diphenyl-2-H-tetrazolium bromide (MTT) solution (5 mg/ml) was added to each well and the cells were incubated for an additional 4 h. Finally, the medium was removed and precipitates were dissolved in 150 μl DMSO with mechanically shaking for 30 min. The absorbance values at the wavelength of 570 nm were collected by the ELX800 microplate reader while $IC_{50}$ values were calculated by using percentage of growth versus untreated control by SPSS (Chicago, IL).

## Result and discussion

### Chemistry

Based on the core scaffold of 5,7-dimethyl-oxazolo[5,4-*d*]pyrimidine-4,6(5*H*,7*H*)-dione, we designed and synthesized 12 novel compounds **N5a–N5l**, and confirmed their chemical structures by $^1$H NMR, IR and MS. For the spectral data on **N5a–N5l**, see the Supplementary Material. Furthermore, the antitumor activities of these compounds were evaluated by using LANCE Ultra TR-FRET and MTT Assay.

The synthetic route is illustrated in Figure 2. The key intermediate of 1,3-dimethyl-5-nitroso-pyrimidine-2,4,6(1*H*, 3*H*, 5*H*)-trione (**2**) was obtained from commercially available 1,3-dimethyl- pyrimidine-2,4,6(1*H*, 3*H*, 5*H*)-trione (**1**) *via* nitrosation with $NaNO_2$ at 81% yield. Reduction of intermediate **2** with $Na_2S_2O_4$ to furnish 1,3-dimethyl-5-amino-pyrimidin-2,4,6(1*H*,3*H*,5*H*)-trione (**3**) at 80% yield, which was subjected to react with various aromatic aldehydes in the presence of ethanol to obtain the corresponding imines (**4a**–**4l**) at 50–70% yield. Cyclization of the imines (**4a**–**4l**) with thionyl chloride provided the target compounds, 5,7-dimethyl-oxazolyl[5,4-d]pyrimidine-4,6 (5*H*,7*H*)-dione derivatives (**N5a–5l**), at 43.2–60.3% yield. All of the synthetic products were isolated by conventional work-up with satisfactory yields. Analytical and spectral data of all synthesized compounds are in full agreement with the proposed structures.

### Compound N5d, N5e and N5f are potent FGFR1 kinase inhibitors

To determine the effect of compounds **N5a–N5l** on FGFR1 kinase activity, we performed LANCE Ultra TR-FRET Assay. As shown in Figure 3, a dose-dependent inhibition was observed for most of the compounds toward FGFR1, among which compounds **N5d**, **N5e**, **N5f** and **N5g** showed highest potency. Importantly, these compounds also exhibited good potency at the concentration of 0.1 and 1 μM comparable to SU5402. We postulate that the result could be due to the space structure of ATP site of FGFR1, which was big enough to contain larger molecules and formed more

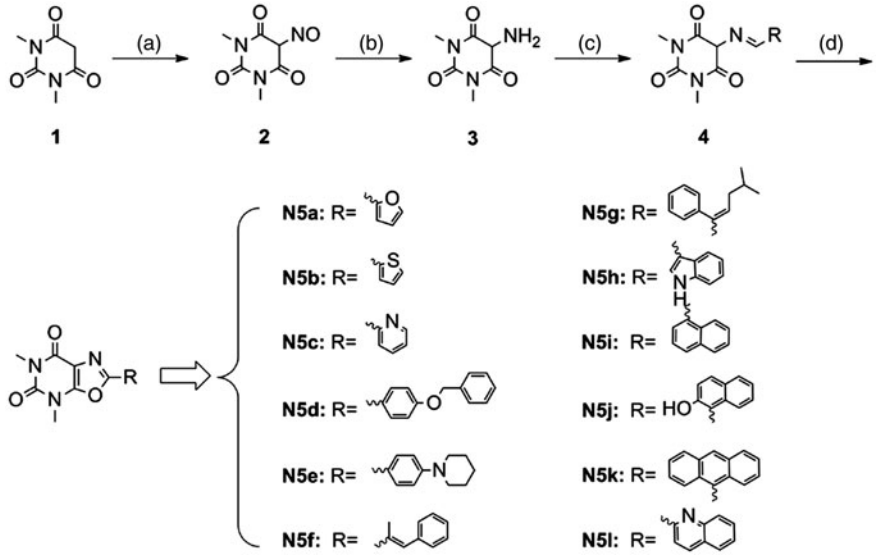


Figure 2. General route for the synthesis of 5,7-dimethyloxazolo[5,4-*d*]pyrimidine-4,6 (5*H*,7*H*)-dione derivatives. Regents and conditions: (a) $NaNO_2$, $CH_3COOH$:$H_2O$ = 1:1, 50 °C, 1 h; (b) $Na_2S_2O_4$, $NH_4OH$, 50 °C, 30 min; (c) R–CHO, $CH_3CH_2OH$, 80 °C, 3 h; (d) $SOCl_2$, 60 °C, 1 h, pH 7.

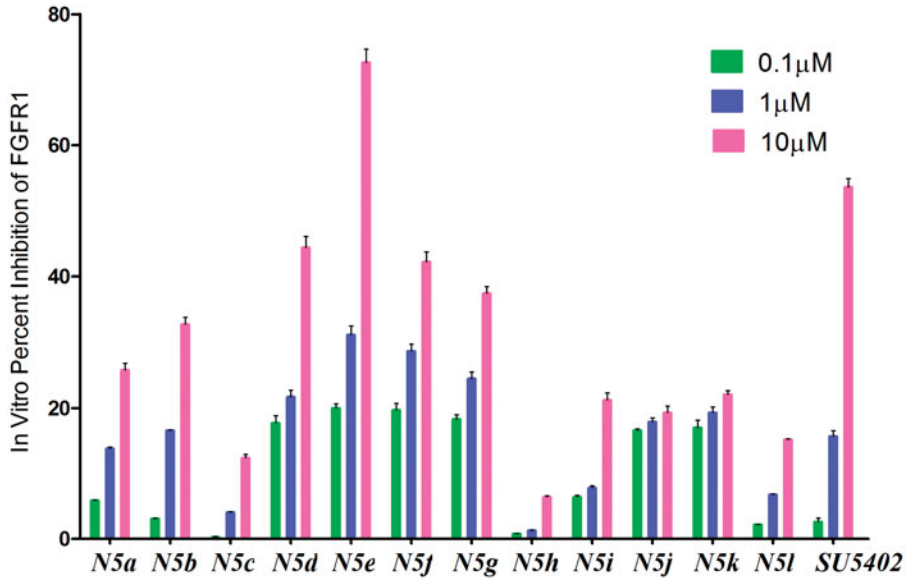


Figure 3. Inhibition of FGFR1 by the tested compounds *in vitro*. The activity of all synthesized compounds at indicated concentrations toward in inhibiting FGFR1 kinase activity was determined by the LANCE Ultra TR-FRET Assay. The data was collected on the EnVision Multilabel Reader and controlled by SPSS.

bonds with these molecules. Among the tested compounds, **N5e** showed the best performance at the concentration of 10 μM, which was more potent than SU5402. The piperidyl group of compound **N5e** appears to be able to form more hydrogen bonds with the ATP site and occupy the hydrophobic pocket with the long side chain. The other compound **N5g** also showed a strong activity to the FGFR1 kinase at a comparable level to the positive control SU5402.

### The antitumor activity of compounds N5a–N5l *in vitro*

These synthesized compounds (**N5a–5l**) were further screened for their antitumor activities *in vitro*. Three cancer cell lines known to express high levels of FGFR1 were tested in MTT assay including the mouse melanoma (B16F10) and human lung cancer (H460 and A549) and the result is summarized in Table 1.

It has been reported that high FGFR1 expression contributes to cell proliferation in both H460 and A549 human lung cancer cells[24,25]. Given that our compounds demonstrated inhibition effect on FGFR1 kinase activity, we performed MTT assay to determine the potential effect on cell proliferation. Out results revealed that several of the compounds showed antitumor activity, which seemingly corresponded to the inhibition of FGFR1 (Table 1). Compounds **N5f**, **N5g**, **N5h** and **N5i** demonstrated promising activity toward nearly all of the three cells (H460, B16F10 and A549). Interestingly, compound **N5g** showed an *in vitro* anticancer activity with $IC_{50}$ values below 6.0 μM, closed

Table 1. The $IC_{50}$ values for the tested compounds on cell proliferation based on MTT assay.

| | $IC_{50}$ (μM) | | |
|---|---|---|---|
| Compound | H460 | B16F10 | A549 |
| **N5a** | 7.9 ± 1.05 | >1000 | >1000 |
| **N5b** | 608.5 ± 18.4 | 311.7 ± 10.1 | 311.9 ± 24.2 |
| **N5c** | >1000 | >1000 | 166.3 ± 16.4 |
| **N5d** | 57.85 ± 2.54 | >1000 | >1000 |
| **N5e** | >1000 | 40.18 ± 1.53 | 424.1 ± 20.13 |
| **N5f** | 21.36 ± 0.53 | 15.26 ± 0.85 | 16.8 ± 1.06 |
| **N5g** | 1.47 ± 0.53 | 4.260 ± 2.61 | 5.837 ± 3.20 |
| **N5h** | 59.8 ± 2.57 | 35.1 ± 0.24 | 29.77 ± 1.03 |
| **N5i** | 57.5 ± 5.67 | 35.6 ± 1.56 | 372.9 ± 2.13 |
| **N5j** | >1000 | >1000 | 132.1 ± 3.58 |
| **N5k** | 10.8 ± 0.34 | 32.8 ± 1.34 | 868.1 ± 12.42 |
| **N5l** | 60.71 ± 1.03 | 292.6 ± 5.41 | 30.94 ± 1.56 |
| **SU5402** | 2.217 ± 2.01 | 1.262 ± 0.960 | 3.483 ± 1.47 |

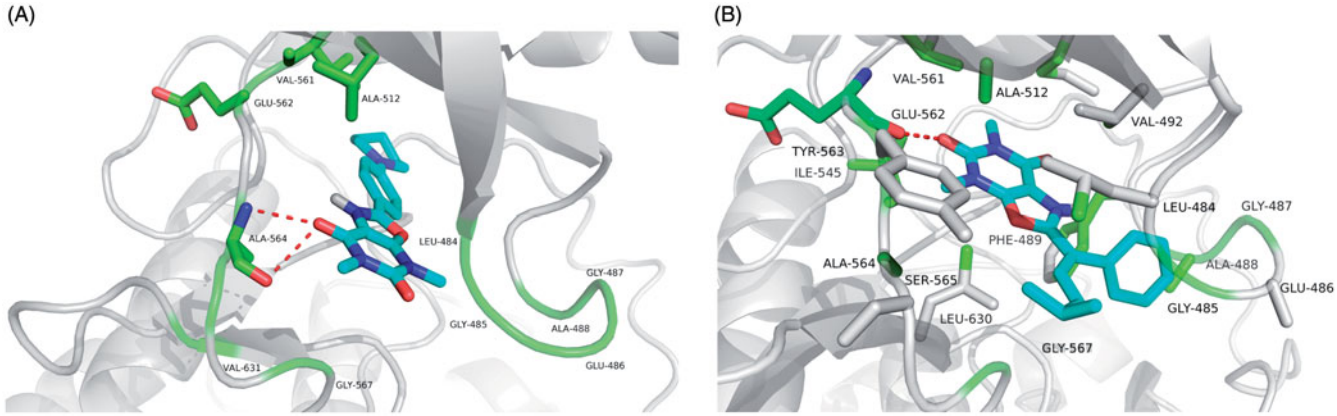


Figure 4. Computed binding geometry of the new inhibitors **N5e** (A) and **N5g** (B) with the FGFR1 ATP-binding pocket.

to that of the positive control drug (SU5402). The reason may be that compound **N5g** has more hydrophobic groups than **N5d–f**, so that the former could be more membrane permeable. Additionally, **N5a** and **N5k** affected only H460 cells, whereas **N5e** showed good activity toward B16F10.

An evident loss in inhibitory activity was observed when the side chain was substituted with a single ring, such as in **N5a**, **N5b** and **N5c**, suggesting that the group is too small to occupy the hydrophobic pocket or form a bond with FGFR1. SAR also demonstrated that the bulky and flexible groups might play the most crucial role both in regulating the kinase activity and the cellular activity. Additionally, the bulky group likely forges a tight link to the hydrophobic pocket to hinder the movement of the compound side chain out of the hydrophobic pocket. Consistent with this, **N5f**, **N5g**, **N5h** and **N5i** exhibit more promising activity.

## Conclusion

To explain the results, we proposed a hypothetical model for **N5g** and **N5e** binding to FGFR1 based on computational docking results (Figure 4). As usual, the oxygen atom of a carbonyl group on **N5g** bound to the hydrogen of GLU562 to form hydrogen bond (distance cutoff: 2.6 Å) in the active pocket, while side chain (*Z*)-(4-methylpent-1-en-1-yl) benzene in the designed compound could be placed into the hydrophobic pocket formed by SER565, PHE489, GLY567, LEU630, LEU484, ALA488, GLY485, GLY487 and GLU486, and generates p–p stacking interactions with the PHE489. The docking of **N5e** to FGFR1 was similar to that of **N5g**, but form two hydrogen bonds (distance cutoff: 3.0 and 3.1 Å) in the pocket. The results of the docking depicted that the energy of the two compounds, **N5e** and **N5g** binding with FGFR1 were similar (8.16 and 7.48 kcal/mol, respectively). Therefore the binding geometry provides potential explanations for the more potent antitumor activity associated with the multiple hybrid compounds.

In summary, 12 novel 5,7-dimethyl-oxazolo[5,4-d]pyrimidine-4,6(5*H*,7*H*)-dione derivatives were designed, synthesized and evaluated for their antitumor activity both in various cancer cells with high FGFR1 kinase activity. Although most compounds showed a linear relationship in inhibiting FGFR1 kinase activity, the compounds **N5e** and **N5g** showed better selectivity toward FGFR1 suggesting that the compounds with side chains substituted with stereo-structure groups exhibited better activity than those with planar structures. We speculate that this could be due to the space structure of FGFR1 ATP pocket, which was big enough to accommodate larger molecules and form more bonds with these molecules.

Varying selectivity toward cancer cell proliferation was observed for these compounds. **N5a** and **N5d** affected only the H460 cells, whereas **N5f**, **N5g**, **N5h** and **N5i** exhibited good activity against all three lines. Among the compounds tested, **N5g** was found to exhibit the most potent and universal anti-proliferative activity in all cancer cell lines similar to the positive drug SU5402. We suggest that the 5,7-dimethyl-oxazolo[5,4-d]pyrimidine-4,6(5*H*,7*H*)-dione derivatives may serve as potential agents for the treatment of FGFR1-mediated cancers. Therefore, **N5g** could be a more promising candidate compound for further modification and anti-tumor activity study.

## Acknowledgements

The IR, $^1$H NMR, ESI-MS and elemental analysis were recorded by the Analysis and Test Center of Wenzhou Medical University.

## Declaration of interest

This work was supported by the National Natural Science Foundation of China (81373262).

## References

1. Van-der-Noll R, Leijen S, Neuteboom GH, et al. Effect of inhibition of the FGFR-MAPK signaling pathway on the development of ocular toxicities. Cancer Treat Rev 2013;39:664–72.
2. Guagnano V, Furet P, Spanka C, et al. Discovery of 3-(2,6-dichloro-3,5-dimethoxy-phenyl)-1-{6-[4-(4-ethyl-piperazin-1-yl)-phenylamino]-pyrimidin-4-yl}-1-methyl-urea (NVP-BGJ 398), a potent and selective inhibitor of the fibroblast growth factor receptor family of receptor tyrosine kinase. J Med Chem 2011;54:7066–83.
3. Takeuchi K, Ito F. Receptor tyrosine kinases and targeted cancer therapeutics. Biol Pharm Bull 2011;34:1774–80.
4. Kottakis F, Polytarchou C, Foltopoulou P, et al. FGF-2 regulates cell proliferation, migration, and angiogenesis through an NDY1/KDM2B-miR- 101-EZH2 pathway. Mol Cell 2011;43:285–98.
5. Turner N, Grose R. Fibroblast growth factor signalling: from development to cancer. Nat Rev Cancer 2010;10:116–29.
6. Gangjee A, Zhao Y, Raghavan S, et al. Design, synthesis and evaluation of 2-amino-4-m-bromoanilino-6-arylmethyl-7H-pyrrolo[2,3-d]pyrimidines as tyrosine kinase inhibitors and antiangiogenic agents. Bioorg Med Chem 2010;18:5261–73.
7. Chen Z, Wang X, Zhu W, et al. Acenaphtho[1,2-b]pyrrole-based selective fibroblast growth factor receptors 1 (FGFR1) inhibitors: design, synthesis, and biological activity. J Med Chem 2011;54:3732–45.
8. Yang F, Zhang Y, Ressler SJ, et al. FGFR1 is essential for prostate cancer progression and metastasis. Cancer Res 2013;73:3716–24.
9. Weiss J, Sos ML, Seidel D, et al. Frequent and focal FGFR1 amplification associates with therapeutically tractable FGFR1

dependency in squamous cell lung cancer. Sci Transl Med 2010;2:62–93.
10. Turner N, Pearson A, Sharpe R, et al. FGFR1 amplification drives endocrine therapy resistance and is a therapeutic target in breast cancer. Cancer Res 2010;70:2085–94.
11. Liang G, Chen G, Wei X, et al. Small molecule inhibition of fibroblast growth factor receptors in cancer. Cytokine Growth Factor Rev 2013;24:467–75.
12. Ravindranathan KP, Mandiyan V, Ekkati AR, et al. Discovery of novel fibroblast growth factor receptor 1 kinase inhibitors by structure-based virtual screening. J Med Chem 2010;53:1662–72.
13. Fearon AE, Gould CR, Grose RP. Int. FGFR signalling in women's cancers. J Biochem Cell Biol 2013;45:2832–42.
14. Dokduang H, Juntana S, Techasen A, et al. Survey of activated kinase proteins reveals potential targets for cholangiocarcinoma treatment. Tumour Biol 2013;34:3519–28.
15. Byron SA, Chen H, Wortmann A, et al. The N550K/H mutations in FGFR2 confer differential resistance to PD173074, dovitinib, and ponatinib ATP-competitive inhibitors. Neoplasia 2013;15:975–88.
16. Patel A, Tiwari AK, Chufan EE, et al. PD173074, a selective FGFR inhibitor, reverses ABCB1-mediated drug resistance in cancer cells. Cancer Chemother Pharmacol 2013;72:189–99.
17. Gryshchenko AA, Levchenko KV, Bdzhola VG, et al. Design, synthesis and biological evaluation of naphthostyril derivatives as novel protein kinase FGFR1 inhibitors. J Enzyme Inhib Med Chem 2014;18:1–7.
18. Skaper SD, Kee WJ, Facci L, et al. The FGFR1 inhibitor PD 173074 selectively and potently antagonizes FGF-2 neurotrophic and neurotropic effects. Neurochem 2000;75:1520–7.
19. Mohammadi M, McMahon G, Sun L, et al. Structures of the tyrosine kinase domain of fibroblast growth factor receptor in complex with inhibitors. Science 1997;276:955–60.
20. Thompson AM, Delaney AM, Hamby JM, et al. Synthesis and structure–activity relationships of soluble 7-substituted 3-(3,5-dimethoxyphenyl)-1,6-naphthyridin-2-amines and related ureas as dual inhibitors of the fibroblast growth factor receptor-1 and vascular endothelial growth factor receptor-2 tyrosine kinases. J Med Chem 2005;48:4628–53.
21. Grand EK, Chase AJ, Heath C, et al. Targeting FGFR3 in multiple myeloma: inhibition of t(4;14)-positive cells by SU5402 and PD173074. Leukemia 2004;18:962–6.
22. Wang Y, Cai Y, Ji J, et al. Discovery and identification of new non-ATP competitive FGFR1 inhibitors with therapeutic potential on non-small-cell lung cancer. Cancer Lett 2014;344:82–9.
23. Kumar SB, Narasu L, Gundla R, Dayam R, JARPS. Fibroblast growth factor receptor inhibitors. Curr Pharm Des 2013;19:687–701.
24. Yang J, Zhao H, Xin Y, Fan L. MicroRNA-198 inhibits proliferation and induces apoptosis of lung cancer cells via targeting FGFR1. J Cell Biochem 2014;115:987–95.
25. Wu X, Huang H, Wang C, et al. Identification of a novel peptide that blocks basic fibroblast growth factor-mediated cell proliferation. Oncotarget 2013;4:1819–28.

**Supplementary material available online**